

AperTO - Archivio Istituzionale Open Access dell'Università di Torino

## The temperature dependence of radiationless transition rates from ab initio computations

### This is the author's manuscript

*Original Citation:*

*Availability:*

This version is available <http://hdl.handle.net/2318/137422> since 2016-10-11T12:43:45Z

*Published version:*

DOI:10.1039/c0cp02307h

*Terms of use:*

Open Access

Anyone can freely access the full text of works made available as "Open Access". Works made available under a Creative Commons license can be used according to the terms and conditions of said license. Use of all other works requires consent of the right holder (author or publisher) if not exempted from copyright protection by the applicable law.

(Article begins on next page)

# The temperature dependence of radiationless transition rates from *ab-initio* computations

Raffaele Borrelli<sup>\*a,b</sup> and Andrea Peluso<sup>\*c</sup>

February 24, 2011

## Abstract

The calculation of radiationless transition rates and of their temperature dependence from first principles is addressed by combining reliable electronic computations of the normal modes of the two electronic states with Kubo's generating function approach for the evaluation of the Franck-Condon weighted density of states. The whole sets of normal modes of the involved cofactors have been employed, taking into account the effects of nuclear equilibrium position displacements, of vibrational frequency changes, and of mixing of the normal modes. Application to the case of the elementary electron transfer step between bacteriopheophytin and ubiquinone cofactors of bacterial photosynthetic reaction centers yields a temperature dependence of the electron transfer rates in very good agreement with the experimental data.

---

<sup>a</sup> *Dipartimento di Chimica, Università di Salerno, I-84084 Fisciano, Salerno, Italy; Tel: 089969593; E-mail: rborrelli@unisa.it*

<sup>b</sup> *Institute of Physical and Theoretical Chemistry, Technical University of Munich, D-85748 Garching, Germany.*

<sup>c</sup> *Dipartimento di Chimica, Università di Salerno, I-84084 Fisciano, Salerno, Italy; Tel: 089969577; E-mail: apeluso@unisa.it*

# 1 Introduction

Radiationless transitions between two electronic states are of outstanding importance in chemistry, since they affect the electronic spectrum of almost all chemicals and control processes of relevant technological and biochemical interest, such as electron transfer (ET) and photoisomerization. Progresses in the area of fluorescent dyes,<sup>1</sup> microelectronics,<sup>2</sup> single-molecule charge transport,<sup>3</sup> and light driven molecular machines<sup>4-6</sup> have led to a crescent demand of computational approaches for obtaining reliable estimates of radiationless transition rates, and, overall, of their temperature dependence, which represents an important piece of information for determining from experimental data the parameters which control transition rates.

The quantum theory of radiationless processes has been developed in the fifties by Lax and Kubo,<sup>7,8</sup> in parallel with Marcus' classical ET theory.<sup>9,10</sup> Those theories, and their extensions,<sup>11</sup> have been extensively applied to determine the rates of chemical reactions, especially in the field of ET in biosystems,<sup>12-15</sup> however in some cases the lack of detailed information about equilibrium geometries, normal modes and vibrational frequencies of the involved molecules had imposed the use of drastic approximations which could limit the possibility of extracting from experimental data the parameters which control transition rates. More refined models for radiationless rates based on the spin-boson theory have also been developed, and widely applied to the study of ET in condensed media.<sup>16-18</sup>

A significant improvement has been provided by Warshel and coworkers, who introduced the dispersed polaron model which, combined with the quantum mechanical consistent force field method (QCFF/PI), and its extensions, has allowed to determine rate constants from classical trajectory simulations.<sup>19-21</sup> Indeed, that methodology has provided deep insights into the role of protein motion on their chemical activity.<sup>22,23</sup> In the dispersed polaron approach the microscopic parameters which drive a radiationless transition, *i.e.* the variations of the equilibrium geometries and vibrational normal modes are usually determined by an *a posteriori* analysis of the autocorrelation function of the energy gap between the electronic states of reactants and products, so that disentangling the various contributions of the nuclear motion to the overall kinetics may become quite

laborious. Nowadays modern computational tools provide the possibility of reliably calculating such parameters both for the ground and the excited states of the molecules, thus opening the way toward the direct calculation of radiationless transition rates from *ab initio* electronic computations.<sup>24-36</sup>

In this paper we present a computational approach which combines use of reliable *ab-initio* computations of molecular equilibrium geometries and vibrational frequencies with Kubo's generating function (GF) method for computing the Franck-Condon weighted density of states. The approach takes into account both the linear and the quadratic coupling terms arising from equilibrium position displacements, mixing of normal modes, and frequency changes, and allows to include in computations the whole set of intramolecular normal modes, thus providing a powerful computational tool for evaluating radiationless transition rates and their temperature dependence. The approach discussed here is valid for those limiting cases of radiationless transitions which can be described by the Fermi Golden Rule (FGR) expression in the harmonic and Condon approximations, however the theory can be easily extended to tackle with problems which go beyond the Condon approximation. Of course it is well known that, in cases of strong electronic coupling the FGR breaks down and dynamical calculations become necessary.<sup>37,39</sup> Application to the case of ET between bacteriopheophytin and ubiquinone occurring in the photosynthetic reaction center (PRC) of *Rhodobacter sphaeroides* shows that the temperature dependence of ET rates is very reliably predicted and the parameters which control ET rates obtained by a best fitting of the experimental data are in very good agreement with those already reported in the literature.

## 2 The Franck-Condon weighted density of states

The Fermi golden rule expression for the rate of radiationless transition between two electronic states is:

$$W = \frac{2\pi}{\hbar} V^2 F(\Delta E, T), \quad (1)$$

where  $V$  is the coupling element, which has been assumed in deriving eq. (1) to be independent of vibrational coordinates, and  $F(\Delta E, T)$  is the Franck-Condon weighted

density of states, given by:

$$F(\Delta E, T) = \sum_{v_g, v_e} \frac{1}{Z(v_g)} e^{-\beta E(v_g)} |\langle v_g | v_e \rangle|^2 \delta(E(v_e) - E(v_g) - \Delta E) \quad (2)$$

where  $E(v_g)$  and  $E(v_e)$  are the energies of the vibrational states of the initial and final electronic state  $|g\rangle$  and  $|e\rangle$ , respectively,  $\Delta E$  is the electronic energy difference between the minimum energy configurations of  $|g\rangle$  and  $|e\rangle$ ,  $\langle v_g | v_e \rangle$  is the Franck-Condon (FC) integral,  $Z(v_g)$  is the vibrational partition function of the electronic state  $|g\rangle$ ,  $\beta = 1/kT$ , and the sum runs over all vibrational states of  $|g\rangle$  and  $|e\rangle$ .

The evaluation of  $F(\Delta E, T)$  for large ET cofactors is not an easy task, even in the harmonic approximation. The calculation of FC integrals by use of multi-index recurrence relations,<sup>40–45</sup> poses problems for the extremely large amount of data which has to be stored, and its direct formulation, originally proposed by Sharp and Rosenstock for two and three simultaneously excited modes,<sup>40</sup> proved to be difficult to implement.<sup>46–49</sup> Data storage problems can be somewhat limited by using algorithms based on an judicious way of choosing normal mode excitations,<sup>44,49–51</sup> and completely overcome by using a perturbative treatment of the normal mode mixing effect,<sup>52</sup> the so called Duschinsky effect.<sup>53</sup> From a computational point of view, the most efficient method for evaluating  $F(\Delta E, T)$  is the generating function approach developed in the fifties by Lax and Kubo.<sup>7,8</sup>

The GF approach is based on the Fourier transformation of the delta function of eq. (2), and on the coordinate representation of the vibrational Hamiltonian operators of the initial and final states,  $\mathcal{H}_g$  and  $\mathcal{H}_e$  in eq. (4) below. In short, the approach consists in *i*): writing  $F(\Delta E, T)$  as the inverse Fourier transform of a correlation function  $f(\tau)$

$$F(\Delta E, T) = \frac{1}{2\pi} \int_{-\infty}^{+\infty} e^{i\Delta E\tau} f(\tau) d\tau, \quad (3)$$

where

$$f(\tau) = \text{Tr}\{e^{-i\tau\mathcal{H}_e} e^{-(\beta-i\tau)\mathcal{H}_g}\} / \text{Tr}\{e^{-\beta\mathcal{H}_g}\}; \quad (4)$$

*ii*) modeling  $\mathcal{H}_g$  and  $\mathcal{H}_e$  in harmonic approximation, with normal modes of vibration ( $\mathbf{Q}_g$  and  $\mathbf{Q}_e$ ) differing for equilibrium positions, frequencies, and directions, and related each other by Duschinsky's transformation:

$$\mathbf{Q}_e = \mathbf{J}\mathbf{Q}_g + \mathbf{K}; \quad (5)$$

iii) integrating over normal modes and performing the trace operation finally give:

$$f(\tau) = [\det \Phi]^{-1/2} \exp(-\tilde{\mathbf{K}}\mathbf{J}\mathbf{T}_g(\mathbf{T}_g + \mathbf{T}_e)^{-1}\mathbf{T}_e\tilde{\mathbf{J}}\mathbf{K}), \quad (6)$$

where

$$\mathbf{T}_g = \boldsymbol{\omega}_g \tanh[(\beta - i\tau)\boldsymbol{\omega}_g/2]; \quad \mathbf{T}_e = \tilde{\mathbf{J}}\boldsymbol{\omega}_e \tanh(i\tau\boldsymbol{\omega}_e/2)\mathbf{J} \quad (7)$$

$$\mathbf{C}_g = \boldsymbol{\omega}_g / \tanh[(\beta - i\tau)\boldsymbol{\omega}_g/2]; \quad \mathbf{C}_e = \tilde{\mathbf{J}}\boldsymbol{\omega}_e / \tanh(i\tau\boldsymbol{\omega}_e/2)\mathbf{J} \quad (8)$$

$$\Phi = [2 \sinh(\beta\boldsymbol{\omega}_g/2)]^{-2}\boldsymbol{\omega}_g^{-1} \sinh[(\beta - i\tau)\boldsymbol{\omega}_g](\mathbf{T}_g + \mathbf{T}_e)(\mathbf{C}_g + \mathbf{C}_e)\boldsymbol{\omega}_e^{-1} \sinh(i\tau\boldsymbol{\omega}_e), \quad (9)$$

$\boldsymbol{\omega}_g, \boldsymbol{\omega}_e$  being the diagonal matrices of the vibrational frequencies of the initial and final states.

The above formulation is very efficient for numerical treatments because the calculation of  $F(\Delta E, T)$  can be recast into a discrete Fourier transform problem

$$F(\Delta E, T) = \frac{1}{N} \sum_{k=1}^N w(\tau_k) f(\tau_k) e^{i\Delta E \tau_k} \quad (10)$$

where  $w(\tau)$  is a proper window function, necessary to avoid boundary and spectral leakage problems.<sup>54</sup>

The appealing feature of the GF approach is in the fact that, at variance with quantum dynamics, its computational cost is independent of the value of the temperature used in calculation, making thus it possible the analysis of the temperature dependence of ET rates between large redox cofactors.

### 3 Temperature dependence of ET rate

Here, we will consider the elementary ET step from bacteriopheophytin (BPh) anion to the primary ubiquinone (Q), one of the best characterized ET step in bacterial PRCs,<sup>55,56</sup> which exhibits a moderate but significant temperature dependence.<sup>57,58</sup> The first pioneering measurements yielded an unusual behavior, with the ET rate increasing about threefold with decreasing temperature in the range between 300 and 25 K, and then decreasing abruptly at temperature below 25 K. In subsequent measurements the abrupt decrease of the rate below 25 K was no longer observed, even though in one series of

measurements, those based on the absorption at 545 nm, corresponding to the bleaching of the  $Q_x$  absorption of BPh, a slight decrease of the rate at 5 K was indeed observed, see fig. 5 of ref 58 and fig. 3.

That non-Arrhenius behavior of ET rates could be attributed either to the electronic coupling factor, which could exhibit a weak T dependence due to conformational changes which allow a shorter contact between the two cofactors at lower temperature,<sup>59</sup> or to the temperature dependence of the FC weighted density of states. Since the latter effect cannot be anyway reasonably neglected, we started by assigning the whole temperature dependence of ET rates to the thermal weighted FC factors.

The rotation matrix  $\mathbf{J}$  and the equilibrium position displacement vector  $\mathbf{K}$ , the main ingredients for the calculation of the thermal weighted FC factors via eq. (1)-eq. (6), have been evaluated using the equilibrium geometries, the normal modes, and the vibrational frequencies of BPh and Q cofactors in their neutral and anionic forms computed at density functional theory level, by using the hybrid B3LYP exchange correlation potential and the 6-311+G\*\* basis set. The native PRC cofactors were modeled by the molecules reported in fig. 1.

insert figure 1

The discrete Fourier transform has been carried out using  $2^{16}$  sampling points with a spacing  $\delta\tau$  chosen to have a resolution  $\delta\omega = \frac{2\pi}{N\delta\tau}$  of  $0.6 \text{ cm}^{-1}$ . These parameters have been determined from Nyquist's theorem on the basis of the overall bandwidth of the expected density of states, and of the desired resolution.<sup>60</sup>

The resulting FC weighted density of states ( $F(\Delta E, T)$ ) as a function of the electronic energy difference between the initial and final state ( $\Delta E = E_i - E_f$ ), computed at different T between 5 and 300 K, are reported in fig. 2. At very low temperature and for lower  $\Delta E$ 's,  $F(\Delta E, T)$  shows peaks characteristic of a system consisting of a discrete set of quantum states superimposed to a continuum, which smoothly rises as  $\Delta E$  rises. As  $\Delta E$  increases,  $F(\Delta E, T)$  becomes a smooth function of the vibrational energy of the final state for all T, exhibiting a broad maximum, which shifts at longer wavenumbers as the temperature increases. The maximum density of states significantly depends on temperature; in the

range  $T=5-70$  K, the maximum falls at wavenumbers  $\omega = 4000 - 4500$   $\text{cm}^{-1}$ , and shifts at  $11000$   $\text{cm}^{-1}$  at  $T=300$  K.

insert figure 2

For  $T$  ranging from 5 to 70 K, the computed  $F(\Delta E, T)$  curves are very close to each other and cross in the region of  $\Delta E$  between  $4500$  and  $5500$   $\text{cm}^{-1}$ , see the inset of fig. 2. Thus in that energy region, assuming that  $\Delta E$  is independent of temperature, the computed ET rates will roughly be temperature independent in the range  $T=5-100$  K, as observed by Kirmaier *et al.*<sup>58</sup> Noteworthy, that value of  $\Delta E$  is fully compatible with the existing experimental data, estimated by delayed fluorescence measurements of isolated reaction centers.<sup>61,62</sup>

The computed temperature dependence of ET rates is reported in fig. 3 together with the experimental results. The computed values have been obtained from the Fermi Golden rule expression (*c.f.* eq. (1)), using the FC weighted densities calculated at the temperatures of the available experimental data, and evaluating the two parameters  $\Delta E$  and  $V$  by a least squares fit. That procedure yields  $\Delta E = 5830$   $\text{cm}^{-1}$  and  $V = 10.0$   $\text{cm}^{-1}$ , the latter in agreement with Kuhn's theoretical estimate ( $10$   $\text{cm}^{-1}$ ), obtained by evaluating the coupling element between the highest occupied and the lowest unoccupied molecular orbitals of the donor and acceptor groups in the Slater potential field.<sup>63</sup> The other two curves reported in fig. 3 have been obtained by setting  $\Delta E$  to  $5400$   $\text{cm}^{-1}$  and  $6200$   $\text{cm}^{-1}$ , and evaluating  $V$  by least squares. The resulting values are  $V = 9.9$   $\text{cm}^{-1}$  for  $\Delta E = 5400$   $\text{cm}^{-1}$  and  $V = 10.1$   $\text{cm}^{-1}$  for  $\Delta E = 6200$   $\text{cm}^{-1}$ .

insert figure 3

The temperature dependence of the ET rates is well reproduced by computations. At lower temperatures there is a close agreement between theoretical and experimental data, the computed rates being within the range of the experimental error reported by Kirmaier *et al.* At higher temperatures, above 250 K, the computed rates are slightly underestimated, suggesting that the role of the surrounding medium in promoting ET dynamics, not considered in the present treatment, but for the adopted values of  $\Delta E$  and  $V$ , becomes more important.



## 4 Discussion

The non-Arrhenius behavior of ET from BPh<sup>-</sup> to Q, characterized by a temperature independent rate up to T=130 K and a rough  $T^{-\frac{1}{2}}$  dependence at higher temperatures, requires a quantum mechanical treatment of the vibrational states of the system. Indeed, Jortner's ET quantum theory predicts a  $T^{-\frac{1}{2}}$  dependence for an activationless ET, a process for which the nuclear potential energy surfaces of the initial and final electronic states cross at the minimum energy configuration of the initial state.<sup>11</sup> The single mode approximation of the multiphonon ET theory, although giving a reasonable qualitative trend of the T dependence of ET rates, failed in reproducing either the temperature at which the rates start to decrease or the exact ratio of rate decreasing.<sup>14,58</sup> Inclusion of a few higher energy quantum modes did not improve the situation. A more satisfying fit of ET rates was obtained by using a slightly modified version of Jortner's quantum theory, including quadratic coupling terms originated by the vibrational frequency changes.<sup>64</sup>

The importance of quadratic coupling terms in ET processes is now well recognized.<sup>65-69</sup> Those terms arise both from normal mode mixing and frequency changes. Frequency changes have an important physical meaning, inasmuch they lead to different densities of vibrational states for the initial and final electronic states, allowing for entropy changes, which make  $\Delta G$  to be a function of temperature. Kirmaier *et. al* assigned the observed temperature dependence of ET rates to a weak temperature dependence of  $\Delta G$ : from the fit of the rates they found a decrease of  $\Delta G$  by 500-1000 cm<sup>-1</sup> as the temperature is lowered from 295 to 100 K.

The generating function approach used here takes into account both the linear and the quadratic coupling terms, *i.e.* equilibrium position displacements, mixing of normal modes, and frequency changes. Disentangling the contribution of each effect to ET rates is not an easy task. In an attempt to understand a little more, we have evaluated the FC weighted density of states at different temperatures including only one effect at a time. Since the effects are not additive, but rather act in a cooperative way (interference between probability amplitudes), that can give just a hint on the importance of each contribution. The results are reported in fig. 4 for T=170 K, and in the inset of fig. 4

for  $T=5$  K. To allow a better judgment, we have also included in fig. 4 the FC weighted density of states obtained by including or removing altogether these effects. fig. 4 clearly shows that equilibrium position displacements play the predominant role, both at  $T=5$  K and at  $T=170$  K, but the effect of normal mode mixing is not negligible. Frequency changes seem to play no role, because the FC weighted densities of states computed by considering only frequency changes are very similar, both at  $T=5$  K and at  $T=170$  K, to those obtained by removing all the effects (at 5 K the FC weighted density of states without both linear and quadratic coupling terms becomes the delta function, not visible in the inset of fig. 4). This is not really true, however; a deeper analysis shows that, because of cooperative effects, the density of states computed including both mixing and equilibrium position displacements of the normal modes (curve d of fig. 4) is significantly different from that obtained by including all the first and second order effects (curve f of fig. 4).

Although all contributions are significant, fig. 4 undoubtedly shows that in a hierarchic order the displacements of the equilibrium position have to be considered first. The most strongly displaced modes of BPh/BPh<sup>-</sup> and Q/Q<sup>-</sup> redox couples, computed at B3LYP/6-311+G\*\* level, are reported in tables 1 and 2, respectively, together with the component of the  $\mathbf{K}$  vector in dimensionless units.

Both cofactors possess several modes whose equilibrium positions are significantly displaced upon ET. These modes cover a wide range of wavenumbers, from 25 to 1800  $\text{cm}^{-1}$ . In the quantum dynamics approach to ET from BPh<sup>-</sup> to Q,<sup>32</sup> low frequency displaced modes were important for achieving tight degeneracy between the initial and final vibronic states, a necessary condition for ET to occur by tunneling. High frequency modes were also very important, especially for the case under consideration, because they made it possible to fill up large electronic energy gaps between the initial and final states with a modest increase in vibrational quantum numbers.

As concerns BPh, there are only two high frequency modes whose equilibrium position is predicted to be slightly displaced, one falling at 1010  $\text{cm}^{-1}$ , the other at 1639  $\text{cm}^{-1}$  in the neutral form. The mode at 1010  $\text{cm}^{-1}$  is an in-plane mode, with main contributions from CC(N)H and CCC bending, which involve almost the whole macrocycle, including the two

inner hydrogens. The other mode at higher wavenumber is also an in-plane vibration, appearing as a breathing motion of the whole macrocycle, with large contribution of the CC stretching, especially those involving the three CH carbons connecting the five-membered rings. The displacements of both modes are modest, having their origin in small variations of bond distances and valence angles of the macrocycle. The most displaced mode of BPh is a low-frequency mode falling at  $39\text{ cm}^{-1}$  in the neutral form. It is an out-of-plane mode, whose large equilibrium position displacement originates from an out-of-plane distortion of the unsaturated carbons of the R1 ring, cf. fig. 1, in the anionic form of BPh. This out-of-plane distortion of  $\text{BPh}^-$  also determines the smaller displacements of several low-frequency modes of the pair  $\text{BPh}/\text{BPh}^-$ .

The minimum energy geometries of the  $\text{Q}^-/\text{Q}$  pair shows larger differences with respect to those of the  $\text{BPh}^-/\text{BPh}$  pair. Indeed, quinone contributes to a larger extent, *ca.*  $3000\text{ cm}^{-1}$ , to the computed reorganization energy, whereas BPh contribution is *ca.*  $1300\text{ cm}^{-1}$ . Both CO bond distances of the two carbonyl groups are significantly elongated in the anion ( $1.27$  vs  $1.22\text{ \AA}$ ), as well as the unsubstituted CC double bond ( $1.37$  vs  $1.33\text{ \AA}$ ), whereas the formally single CC bonds are significantly shortened ( $1.44$  vs  $1.49\text{ \AA}$ ). The CO bond distances between the ring carbons and the methoxy oxygens are also elongated in the anion ( $1.38$  vs  $1.34\text{ \AA}$ ), and the COC valence angle is significantly smaller ( $116$  vs  $121$  degrees). All these significant geometry distortions lead to several high and low frequency vibrations whose equilibrium positions are significantly displaced. The low frequency displaced modes are mainly torsional motions; the two lowest ones involve torsions of the two methoxyl groups coupled to a libration motion of the whole ring, whereas the higher frequency one corresponds to torsions of the two methyl groups. Among the high frequency displaced modes, the most displaced one falls at  $460\text{ cm}^{-1}$  in the neutral form and corresponds to a breathing motion of the whole ring including all heavy atoms, then there is a mode at  $1174\text{ cm}^{-1}$ , corresponding to a CCH bending including both ring and methyl hydrogens, and other two modes mainly attributable to CO stretchings, falling at  $1703$  and  $1715\text{ cm}^{-1}$  in the neutral form.

insert tables 1 and 2

None of these displaced modes appear to play a predominant role. Several tests carried

out by setting some of the normal mode equilibrium position displacements to zero did not allow for recognition of one or more dominant modes. The same situation was found in studying the dynamics of ET process at  $T=0$  K by numerically solving the time dependent Schrödinger equation. It came out that all the most displaced modes of the two cofactors play a role in the vibronic transition.<sup>32,70</sup> The only mode recurrently populated, often with more than one quantum, was the highly displaced mode of Q predicted at  $460\text{ cm}^{-1}$  by B3LYP/6-311+G\*\*, see table 2, and, because of the high  $\Delta E$ , the excess energy was always taken up by some high-frequency displaced modes of Q and, to a lesser extent, of BPh too.

## 5 Conclusion

In this paper we have shown that, within the limits of applicability of the Fermi Golden rule, the generating function approach by Kubo and Toyozawa combined with reliable computations of the equilibrium geometries and normal modes of the involved electronic states yield an efficient and powerful tool for studying the temperature dependence of the rates of nonradiative transitions, which allows for disentangling from experimental data other important parameters, such as the electronic coupling factor and the energy difference between the involved electronic states, which are not easily obtained by computations in the case of large size biosystems. The approach proposed here is able to take into account both the linear coupling terms, arising from nuclear equilibrium position displacements, and the quadratic ones, which depend on normal mode mixings and frequency changes. The test case we have considered here indicates that all these effects play a role. The elementary electron transfer step from  $\text{BPh}^-$  to Q is characterized by the existence of a multitude of parallel reaction channels, provided by the excitations of low and high frequency intramolecular vibrations of the two redox cofactors. Linear coupling terms appear to play a major role, but quadratic coupling terms are not negligible.

The computational approach used here could be easily implemented within the commercially available packages for electronic calculations, providing a helpful tool for experimentalists working in the field of nonradiative transition; indeed the electronic coupling

factor ( $10\text{cm}^{-1}$ ) and the energy difference between the two electronic states ( $\approx 0.7$  eV) obtained by the best fitting of the experimental data are in very good agreement with those previously reported in the literature.

## 6 Computational details

The equilibrium geometries and the vibrational frequencies of BPh, BPh<sup>-</sup>, Q and Q<sup>-</sup> have been computed with density functional theory using the Becke three parameters functional for the exchange part, and the Lee-Yang-Parr functional for the correlation (B3LYP).<sup>71</sup> In all calculations the standard Pople basis set 6-311+G\*\* has been used. All calculations have been performed with the Gaussian09 package.<sup>72</sup>

Kubo's GF method has been implemented in a locally modified version of the MolFC software.<sup>73</sup>

## 7 Acknowledgment

The financial support of the University of Salerno is gratefully acknowledged. R.B. thanks the Deutsche Forschungsgemeinschaft for a research grant for his staying at the Technische Universität München.

## References

- [1] M. Y. Berezin and S. Achilefu, *Chem. Rev.*, 2010, **110**, 2641–2684.
- [2] C. Joachim, J. K. Gimzewski, and A. Aviram, *Nature*, 2000, **408**, 541–548.
- [3] A. Nitzan, *Ann. Rev. Phys. Chem.*, 2001, **52**, 681–750.
- [4] R. Ballardini, V. Balzani, A. Credi, M. T. Gandolfi, and M. Venturi, *Acc. Chem. Res.*, 2001, **34**, 445.
- [5] D. Gust, T. A. Moore, and A. L. Moore, *Acc. Chem. Res.*, 2001, **34**, 40–48.
- [6] G. Kodis, Y. Terazono, P. Liddell, J. Andreasson, V. Garg, T. A. Hamburger, M. Moore, A. L. Moore, and D. Gust, *J. Am. Chem. Soc.*, 2006, **128**, 1818–1827.
- [7] M. Lax, *J. Chem. Phys.*, 1952, **20**(11), 1752–1760.
- [8] R. Kubo and Y. Toyozawa, *Prog. Theor. Phys.*, 1955, **13**, 160–182.
- [9] R. A. Marcus, *J. Chem. Phys.*, 1956, **24**, 966–978.
- [10] R. A. Marcus, *J. Chem. Phys.*, 1984, **81**, 4494.
- [11] J. Jortner, *J. Chem. Phys.*, 1976, **64**, 4860.
- [12] H. Sumi and R. A. Marcus, *J. Chem. Phys.*, 1986, **84**, 4894–4914.
- [13] M. Bixon and J. Jortner, *Adv. Chem. Phys.*, 1999, **106**, 35–203.
- [14] M. Bixon and J. Jortner, *J. Phys. Chem.*, 1986, **90**, 3795–3800.
- [15] J. Jortner, *Biochim. Biophys. Acta, Bioener.*, 1980, **594**(4), 193–230.
- [16] A. J. Leggett, *Phys. Rev. B*, 1984, **30**, 1208.
- [17] D. Xu and K. Schulten, *Chem. Phys.*, 1994, **182**, 91–117.
- [18] J. S. Bader, R. A. Kuharski, and D. Chandler, *J. Chem. Phys.*, 1990, **93**(1), 230.
- [19] A. Warshel and M. Karplus, *J. Am. Chem. Soc.*, 1972, **94**(16), 5612–5625.

- [20] A. Warshel and M. Levitt, *J. Mol. Biol.*, 1976, **103**(2), 227–249.
- [21] J. K. Hwang and A. Warshel, *Chem. Phys. Lett.*, 1997, **271**(4-6), 223–225.
- [22] A. Warshel and W. W. Parson, *Quarterly Reviews of Biophysics*, 2001, **34**(04), 563–679.
- [23] M. H. M. Olsson, W. W. Parson, and A. Warshel, *Chem. Rev.*, 2006, **106**(5), 1737–1756.
- [24] E. Lee, E. S. Medvedev, and A. A. Stuchebrukhov, *J. Chem. Phys.*, 2000, **112**, 9015.
- [25] J. Tang, M. T. Lee, and S. H. Lin, *J. Chem. Phys.*, 2003, **119**(14), 7188–7196.
- [26] J. R. Reimers and N. S. Hush, *J. Chem. Phys.*, 2003, **119**(6), 3262.
- [27] R. Ianculescu and E. Pollak, *J. Phys. Chem. A*, 2004, **108**(39), 7778–7784.
- [28] J. R. Reimers and N. S. Hush, *J. Am. Chem. Soc.*, 2004, **126**, 4132–4144.
- [29] W. W. Parson and A. Warshel, *Chem. Phys.*, 2004, **296**, 201–216.
- [30] W. W. Parson and A. Warshel, *J. Phys. Chem. B*, 2004, **108**(29), 10474–10483.
- [31] H. Hwang and P. Rossky, *J. Phys. Chem. B*, 2004, **108**(21), 6723–6732.
- [32] R. Borrelli, M. Di Donato, and A. Peluso, *Biophys. J.*, 2005, **89**, 830–841.
- [33] R. Borrelli, M. Di Donato, and A. Peluso, *Theor. Chem. Acc.*, 2007, **117**, 957–967.
- [34] R. Borrelli, M. DiDonato, and A. Peluso, *J. Chem. Theory Comput.*, 2007, **3**, 673–680.
- [35] Q. Peng, Y. Yi, Z. Shuai, and J. Shao, *J. Chem. Phys.*, 2007, **126**(11), 114302–8.
- [36] Q. Peng, Y. Yi, Z. Shuai, and J. Shao, *J. Am. Chem. Soc.*, 2007, **129**(30), 9333–9339.
- [37] A. Raab, G. A. Worth, H.-D. Meyer, and L. S. Cederbaum, *J. Chem. Phys.*, 1999, **110**, 936–946.

- [38] M. Ben-Nun and T. J. Martínez, *Chem. Phys.*, 2000, **259**, 237–248.
- [39] A. Viel, R. P. Krawczyk, U. Manthe, and W. Domcke, *J. Chem. Phys.*, 2004, **120**, 11000–11010.
- [40] T. E. Sharp and K. M. Rosenstock, *J. Chem. Phys.*, 1964, **41**, 3453–3463.
- [41] A. Warshel and M. Karplus, *Chem. Phys. Lett.*, 1972, **17**, 7–14.
- [42] E. V. Doktorov, I. A. Malkin, and V. I. Man'ko, *J. Mol. Spec.*, 1977, **64**, 302–326.
- [43] A. Peluso, F. Santoro, and G. Del Re, *Int. J. Quant. Chem.*, 1997, **63**, 233–244.
- [44] A. Hazra and M. Nooijen, *Int. J. Quantum Chem.*, 2003, **95**(4-5), 643–657.
- [45] R. Borrelli and A. Peluso, *J. Chem. Phys.*, 2003, **119**, 8437–8448.
- [46] V. I. Baranov, L. A. Gribov, and B. K. Novosadov, *J. Mol. Struct.*, 1981, **70**, 1–29.
- [47] D. W. Kohn, E. S. J. Robles, C. F. Logan, and P. Chen, *J. Phys. Chem.*, 1993, **97**, 4936–4940.
- [48] R. Islampour, M. Dehestani, and S. H. Lin, *J. Mol. Spectrosc.*, 1999, **194**, 179–184.
- [49] H.-C. Jankowiak, J. L. Stuber, and R. Berger, *J. Chem. Phys.*, 2007, **127**, 234101–23.
- [50] M. Dierksen and S. Grimme, *J. Chem. Phys.*, 2005, **122**, 244101–9.
- [51] F. Santoro, R. Improta, A. Lami, J. Bloino, and V. Barone, *J. Chem. Phys.*, 2007, **126**(8), 084509.
- [52] R. Borrelli and A. Peluso, *J. Chem. Phys.*, 2008, **129**(6), 064116–7.
- [53] F. Duschinsky, *Acta Phisicochim. URSS*, 1937, **7**, 551–566.
- [54] F. Harris, *Proc. IEEE*, 1978, **66**(1), 51–83.
- [55] M. R. Gunner and L. P. Dutton, *J. Am. Chem. Soc.*, 1989, **111**, 3400–3412.



- [56] M. R. Gunner, D. E. Robertson, and P. L. Dutton, *J. Phys. Chem.*, 1986, **90**, 3783–3795.
- [57] C. C. Schenck, W. W. Parson, D. Holten, M. W. Windsor, and A. Sarai, *Biophys. J.*, 1981, **36**, 479–489.
- [58] C. Kirmaier, D. Holten, and W. W. Parson, *Biochim. Biophys. Acta*, 1985, **810**, 33–48.
- [59] C. Kirmaier and D. Holten, *Proc. Natl. Acad. Sci. USA*, 1990, **87**(9), 3552–3556.
- [60] H. Nyquist, *Bell System Technical Journal*, 1932, **11**, 126–147.
- [61] H. Arata and W. W. Parson, *Biochim. Biophys. Acta*, 1981, **636**, 70.
- [62] H. Arata and W. W. Parson, *Biochim. Biophys. Acta, Bioener.*, 1981, **638**(2), 201–209.
- [63] H. Kuhn, *Phys. Rev. A*, 1986, **34**, 3409–3425.
- [64] T. Kakitani and H. Kakitani, *Biochim. Biophys. Acta, Bioener.*, 1981, **635**(3), 498–514.
- [65] R. Islampour and S. H. Lin, *J. Phys. Chem.*, 1991, **95**(25), 10261–10266.
- [66] A. M. Mebel, M. Hayashi, K. K. Liang, and S. H. Lin, *J. Phys. Chem. A*, 1999, **103**, 10674–10690.
- [67] D. V. Matyushov and G. A. Voth, *J. Chem. Phys.*, 2000, **113**(13), 5413.
- [68] D. W. Small, D. V. Matyushov, and G. A. Voth, *J. Am. Chem. Soc.*, 2003, **125**(24), 7470–7478.
- [69] K. F. Freed, *J. Phys. Chem. B*, 2003, **107**(38), 10341–10343.
- [70] A. Peluso, *Curr. Org. Chem.*, 2010, **14**, 90–105.
- [71] A. D. Becke, *Phys. Rev. A*, 1988, **38**, 3098.

- [72] M. J. Frisch, G. W. Trucks, H. B. Schlegel, G. E. Scuseria, and M. A. R. *et al.*, Gaussian 09 Revision A.1.
- [73] R. Borrelli and A. Peluso, MolFC: A program for Franck-condon integrals calculation, package available at the web-page <http://www.theochem.unisa.it>.

**Table 1** Progressive normal mode number, wavenumbers ( $\text{cm}^{-1}$ ), and dimensionless displacements, of the most displaced normal modes of the pair  $\text{BPh}^-/\text{BPh}$ .

Mode	wavenumber		<b>K</b>
	BPh	$\text{BPh}^-$	
1	30.6	20.0	0.485
2	39.7	35.2	1.042
3	58.2	56.8	0.197
6	92.2	96.7	-0.304
10	135.7	140.6	0.420
11	146.5	147.3	0.967
19	273.0	272.1	0.320
68	1011.9	1010.4	0.404
114	1644.5	1639.3	-0.365

**Figure 1** The structures of the molecules employed for modeling native BPh, and UQ cofactors

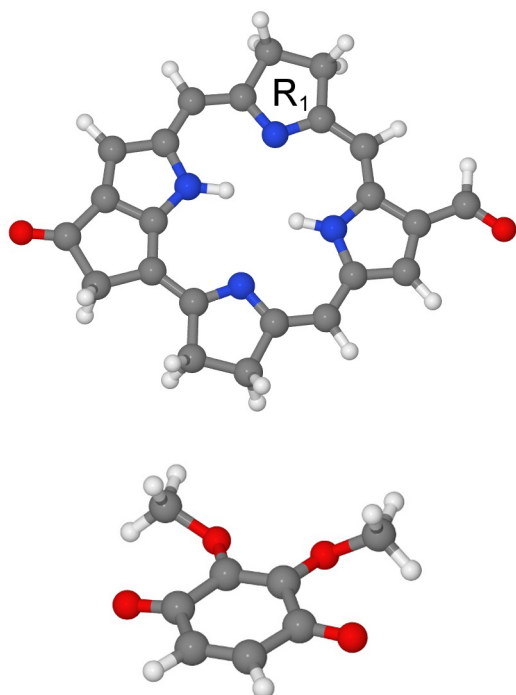


**Table 2** Progressive normal mode number, wavenumbers ( $\text{cm}^{-1}$ ), and dimensionless displacements, of the most displaced normal modes of the pair  $Q/Q^-$

Mode	wavenumber		<b>K</b>
	$Q^-$	$Q$	
1	75.8	42.3	4.801
4	126.8	82.1	-1.097
5	147.2	156.0	1.238
9	319.0	267.3	0.314
12	367.2	377.8	-0.436
13	421.4	406.6	-0.691
15	474.2	460.0	1.490
25	995.8	1003.6	0.318
30	1168.0	1174.3	-0.728
32	1214.1	1228.2	-0.404
41	1486.6	1495.9	-0.460
45	1537.0	1703.9	0.720
46	1635.4	1715.3	0.832

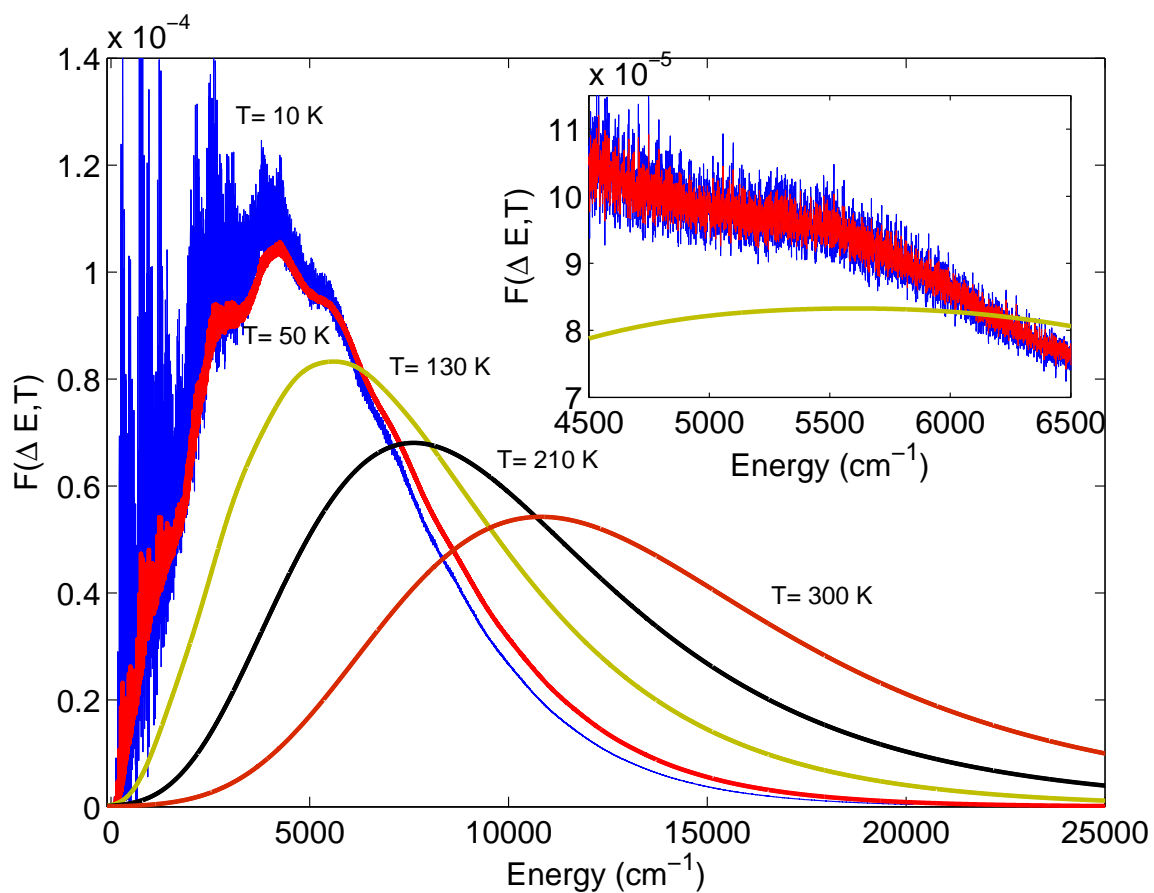


**Figure 2** Franck-Condon weighted density of states for ET from  $\text{BPh}^-$  to UQ as a function of the electronic energy difference between the initial and final state. Inset: magnification of the most interesting energy region.

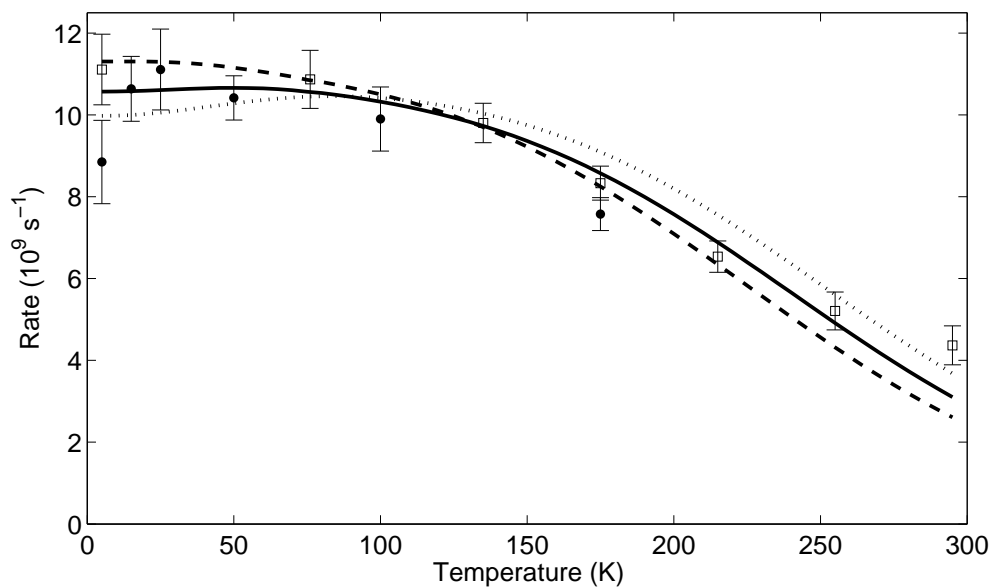


**Figure 3** Computed (lines) and observed temperature dependence of ET rates. Circles and squares refer to measurements at 545 nm and 665 nm, respectively. Computed curves:  $\Delta E = 5400 \text{ cm}^{-1}$  (dashed line),  $\Delta E = 6200 \text{ cm}^{-1}$  (dotted line),  $\Delta E = 5830 \text{ cm}^{-1}$  (full line). Experimental values are taken from ref. 58

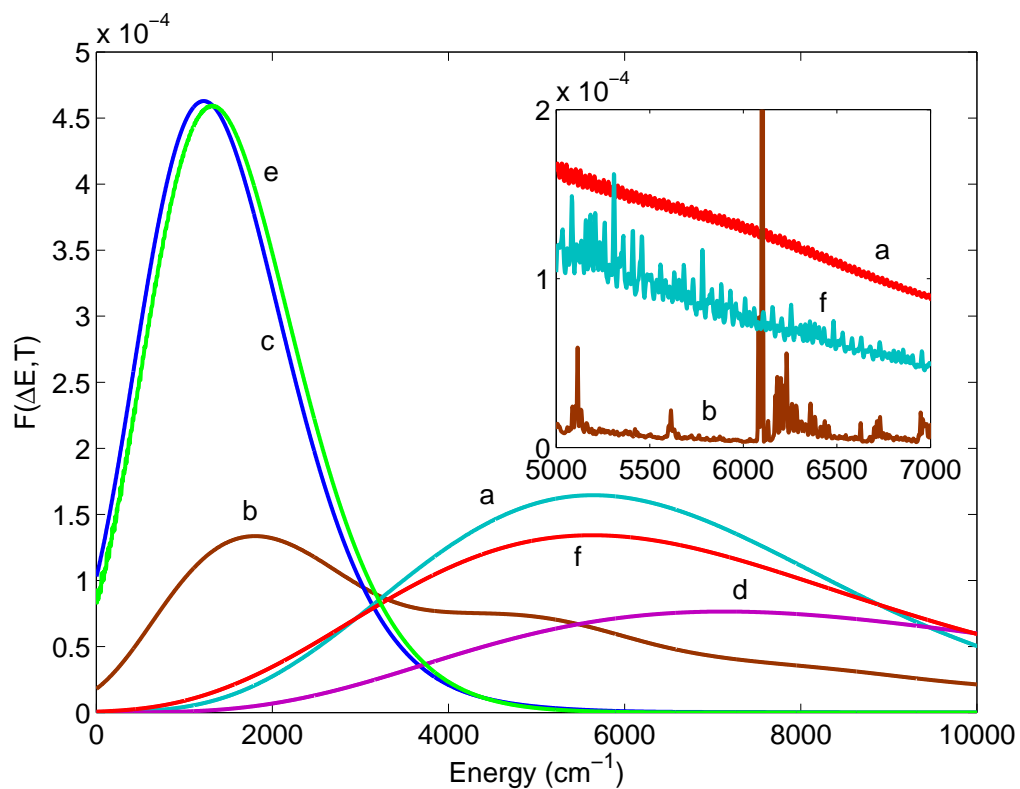


**Figure 4** Franck-Condon weighted densities of states at  $T=170$  K obtained by including one effect at a time: only displaced modes (a), only rotated modes (b), only frequency changes (c), only displaced and rotated modes (d), no effects at all (e), all effects (f). Inset: the same for  $T=5$  K and only for the wavenumber region of interest for ET.